

Development of a simulation–optimization model for multiphase systems in the subsurface: a challenge to real-world simulation–optimization

Kenichiro Kobayashi, Reinhard Hinkelmann and Rainer Helmig

ABSTRACT

The main purpose of this paper is to demonstrate the capability of a new simulation–optimization model especially tailored to investigate the optimal management strategy of a closed coal mine in the Ruhr, Germany. This paper deals with the multiphase/multicomponent flow simulation; the optimization model (simulated annealing); the mesh generation function; the coupling of them; and the use of a parallel computer. Firstly, a mesh generation function is included in the total procedure for the modelling of complex system configurations often required when the real-world problem is dealt with. The multiphase/multicomponent flow simulator can simulate not only groundwater flow and a tracer in it but also the multiphase systems (e.g. gas–water, gas–water–NAPL system). Moreover, a parallelization strategy for the optimization procedure is proposed and implemented to overcome the enormous CPU time problem always tagged to real-world simulation–optimizations. This strategy succeeded in enhancing the efficiency of the overall procedure almost linearly by the number of the processors in a parallel computer. This model is then applied to study how to install the passive extraction wells for controlling the migration of methane continuously desorbed from coal seams inside the closed coal mine in the Ruhr, Germany. The general rule proposed as the result of the application is rather simple although it is considered very useful in many practices of coal mining operations. This paper briefly outlines the overall procedure.

Key words | mesh generation, methane, parallelization, simulation–optimization, single/multiphase flow

INTRODUCTION

For the past couple of decades, the mining sector has played a major role in energy production all over the world. The importance of coal-mining activities can be seen in the fact that, in 1951, the European Coal and Steel Community was established which became an origin of the current European Union. However, the mining sector has been forced to change its role due to the replacement of coal by petroleum as the main energy source. This kind of change has led to the closure of many coal mines in industrialized countries.

Even after the closures, methane still adsorbed in the unexploited coal seams is continuously released into the

abandoned coal mine. Methane emission close to residential areas is dangerous because the accumulation of such methane in houses often causes human health problems. Methane presents a fire and explosion risk, as well as a greenhouse gas whose effect is considered to be dozens of times more potent than that of carbon dioxide. Methane emission causes fewer problems while mines are in operation since it is carefully controlled by gas ventilation. However, closures often lead to the termination of the dewatering and degassing facilities, and thus the risks by less-controlled methane increase. On the other hand,

Kenichiro Kobayashi (corresponding author)
Institute of Sustainability Science,
Kyoto University,
Uji, Kyoto 611-0011,
Kyoto,
Japan
Tel.: +81 774 384541
Fax: +81 774 384546
E-mail: kobayashi.kenichiro@iss.iae.kyoto-u.ac.jp

Reinhard Hinkelmann
Institut für Bauingenieurwesen,
Fachgebiet Wasserwirtschaft und
Hydrosystemmodellierung,
Technische Universität Berlin,
Gustav-Meyer-Allee 25, D-13355 Berlin,
Germany

Rainer Helmig
Institut für Wasserbau, Lehrstuhl für
Hydromechanik und Hydrosystemmodellierung,
Universität Stuttgart, Pfaffenwaldring 61,
D-70550 Stuttgart,
Germany

methane is expected to be utilized as an energy source if the flow is large enough and controlled suction is possible.

Hence, as a matter of course, the primary concern of many coal mine administrators is how to maximize the benefit from the existence of the methane and minimize the danger from it. Toward realizing this goal, several studies on the methane migration processes in the subsurface of coal mines have been carried out over the last couple of years (see e.g. Kobayashi *et al.* 2003; Hinkelmann *et al.* 2004; Hinkelmann 2005).

What is called a simulation–optimization model generally stands for a simulation model coupled with an optimization model and vice versa. Although this kind of simulation–optimization model can be used in several ways for different purposes, one of the most conventional ways among the possible scenarios is probably to use the model as a tool to support the decision-making, e.g. for the selection of an optimal management strategy in some engineering work. Along this line, in this research a simulation–optimization model was developed and applied to a coal mining site in the Ruhr, Germany. The main purpose is to examine the optimal installation of gas extraction wells in the mine in order to control the non-expectable migration of the methane continuously desorbed from the coal seams and released to the surface.

The outline of this paper is as follows. A brief literature survey described in the next section will delineate the distinct aspect of the application in this paper. The next section explains the methods used later in the application. These explanations start from the so-called multiphase model concepts, the optimization model, the coupling procedure of the afore-mentioned simulation model with the optimization model, and finally the parallelization scheme for the optimization procedure. Afterwards, the application of the simulation–optimization model especially designed for the closed coal mining in the Ruhr, Germany is dealt with. In the final section, the conclusion is described.

LITERATURE REVIEW

There are, as it seems, a relatively large number of publications dealing with the simulation–optimization

application when the simulator is a groundwater model. For instance, Zheng (1990) has developed the model called ModGA. In ModGA, the simulation itself is carried out by the groundwater model MODFLOW (McDonald & Harbaugh 1988) and the transport model MT3D. The coupled optimization algorithm is a global search method Genetic Algorithm. Recent publications using MODFLOW can be found in, for example, Maskey *et al.* (2002) or McPhee & Yeh (2004). Maskey *et al.* applied MODFLOW, the particle tracking model (MODPATH) and a global optimization tool, the so-called GLOBE. The purpose of the application is to optimize the groundwater remediation strategy at a site located along the River Elbe in Europe. The work by McPhee & Yeh deals with the groundwater pumping and recharge policies in semiarid regions, specifically the Upper San Pedro River Basin, Arizona, in the USA. Separately from MODFLOW, for example, Nunes *et al.* (2004) deal with the reduction of the redundant groundwater monitoring wells. They set up three different objective functions to select the best subset of the groundwater monitoring stations in a hypothetically created square grid monitoring network. There are some other applications using the so-called optimization packages. These optimization packages contain some optimization algorithms with input/output interfaces capable of being connected to interfaces of other simulation models. Such examples are, for example, ASAP by Aly & Peralta (1999), PEST by Doherty (2002) and UCODE by Poeter & Hill (1998). Meanwhile, far fewer references can be found in respect of multiphase/multicomponent simulators. Some of the few relevant works are found in, for example, Finsterle & Pruess (1995) and Finsterle (2000).

Although the number of simulation–optimization model applications is gradually increasing and the knowledge in theory has been steadily accumulated, the applications to real-world problems, especially those with complex geometries, are still very limited. This is mainly because the simulation model itself requires generally large CPU times when a real-world problem is dealt with; nevertheless, the optimization algorithms, especially global search methods, require quite a few iterations by its nature, i.e. an enormous total CPU time equal to the CPU time of individual real-world simulations multiplied by the number of iterations is always required. This tendency becomes

more prominent when a multiphase model is dealt with as the CPU time generally increases. To overcome this aspect, the development of parallelization designs both in terms of simulation and optimization algorithms has been progressing rapidly to enhance the computational efficiency.

Overall, it is a great challenge to develop simulation–optimization models for the management of subsurface multiphase systems in the actual world. Bearing these facts in mind, a simulation–optimization model capable of dealing with, almost automatically, mesh generation, single/multiphase flow simulation, optimization and parallelization is developed.

METHODS

Model concepts for the methane migration simulations in porous media

A consideration for selecting a model concept for the methane migration simulation in a coal mine is briefly outlined in this section. Attention should be paid so that the focus of the consideration is always put on how to simulate methane-gas migration, and the methane-gas factor always remains in the model concept. This is different from the case when the main attention is given to groundwater flow.

In the saturated zone, it is natural to consider two phases, a liquid and a gas phase, i.e. two-phase type models are used. Suppose that the gas phase is composed of mostly methane, then using a two-phase (liquid, gas) model without including the mass transfer processes between the phases could be appropriate to describe the relevant processes (e.g. Helmig 1997). If it is assumed that the mass transfers between the phases are not of minor importance, then, for example, a two-phase (liquid, gas)/two-component (water, methane) model may be considered as the model one stage higher in terms of the process inclusion. By this model concept, the mass transfers caused by, for example, the dissolution of methane into the liquid phase can be considered (e.g. Helmig *et al.* 2000). However, these models might not yet be appropriate enough when the gas phase consists not only of methane and water vapor but also of some amount of air (e.g. 60% methane, 35% air and 5%

water vapor). Then, a two-phase (liquid, gas)/three-component (water, methane, air) model is expected to be used (Kobayashi *et al.* 2003).

Meanwhile, the first question in modeling the unsaturated zone might be whether the liquid water is to be considered or not. If this is the case, a two-phase-type model is expected to be used again. The choice of a two-phase model among various alternatives (e.g. two-phase, two-phase/two-component, two-phase/three-component model, etc.) is mostly based on the same consideration as for the saturated zone. However, when water in a liquid phase is in a residual-water saturation state, then it could be appropriate to neglect the liquid phase, thereby using one-phase type models could be valid. For example, a one-phase (gas)/two-component (methane, water vapor) model or a one-phase (gas)/three-component (air, methane, water vapor) model can be considered instead. The selection between these two models mainly depends on whether or not the methane component should be distinguished from the air component.

After all, many alternatives can be considered just for the simulation of the methane-migration processes in the subsurface. Thereby, a comparative study between a two-phase (liquid, gas) and a two-phase (liquid, gas)/three-component (air, methane and water) model was carried out to obtain some insight into the differences of the simulation results due to the differences of the model concepts. The focus was put especially on the amount of methane dissolved in the saturated subsurface (Kobayashi 2004). Based on the results of the comparative study, the two-phase/three-component model is selected for the following application, bearing later applications in mind as the groundwater rebound and/or rainfall recharge take place.

Two-phase/three-component model

A schematic diagram of the two-phase (liquid, gas)/three-component (water, methane, air) model concept is shown in Figure 1. In this model concept, there are two immiscible phases, a liquid phase and a gas phase, both of which consist of three components: water, air and methane. Three mass conservation equations derived with regard to the

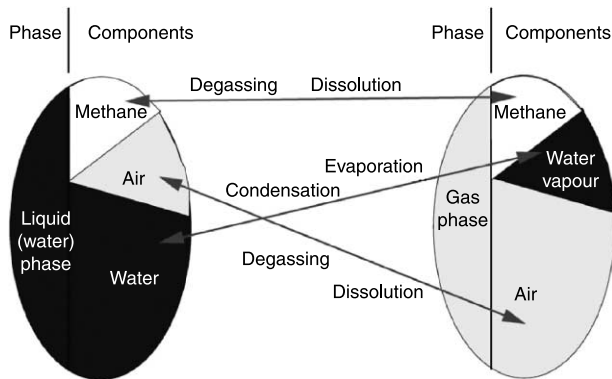


Figure 1 | Schematic diagram of the two-phase/three-component model.

three components are expressed as follows:

$$\frac{\partial (\sum_{\alpha} \phi_{\alpha} \rho_{\alpha}^{mol} x_{\alpha}^{\kappa} S_{\alpha})}{\partial t} + \sum_{\alpha} \nabla \cdot (\rho_{\alpha}^{mol} x_{\alpha}^{\kappa} v_{\alpha}) + \sum_{\alpha} \nabla \cdot (-\rho_{\alpha}^{mol} \mathbf{D}_{\alpha}^{\kappa} \nabla x_{\alpha}^{\kappa}) = q^{\kappa}$$

in $\Omega \times I, \quad \alpha = w, g \quad \kappa = w, m, a,$

where the subscript α denotes the liquid (water) phase (w) and the gas phase (g), while the superscript κ represents the three components, water (w), air (a) and methane (m) (henceforth the liquid phase is often called the water phase since the liquid phase is mostly occupied by the liquid water). ρ_{α}^{mol} stands for the molar density [mol/m^3], x_{α}^{κ} the mole fraction [-], $\mathbf{D}_{\alpha}^{\kappa}$ the diffusion coefficient [m^2/s] and q^{κ} the source/sink term [$\text{mol}/\text{m}^3\text{s}$]. The velocity vector v_{α} is given by the so-called generalized Darcy's law:

$$v_{\alpha} = -\frac{k_{r\alpha}}{\mu_{\alpha}} \mathbf{K} (\nabla p_{\alpha} - \rho_{\alpha}^{mass} \mathbf{g}),$$

where ρ_{α}^{mass} is the mass density [kg/m^3].

With this model concept, mass transfer processes between the phases, i.e. the dissolution and degassing of the air and methane in and out of the water phase, the evaporation of the liquid water to the gas phase and the condensation of the water vapor to the liquid water can be dealt with. This two-phase/three-component module is appended to the MUltiphase Flow, Transport and Energy – Unstructured Grid simulation framework (hereinafter referred to as MUFTE-UG). For further details, see, for example, Kobayashi (2004).

Optimization model

In this type of simulation–optimization approach, the objective function values are calculated as the result of a series of numerical simulations driven by different initial parameter sets. Another way of saying this is that it is, in principle, not possible to delineate the shape of the objective function in advance of having carried out these simulations. However, by conducting some preliminary test simulations using some simpler system configurations of similar kinds, it was anticipated that there would exist multiple local extrema in the eventually formed objective function of the following application, although it does not change the fact that the exact shape cannot be known *a priori*. These preliminary considerations gave the impression that it is not certain whether the derivative-type optimization algorithm can reduce the number of simulation iterations since a reasonable initial guess is not necessarily possible for the following application due to lack of information. A note would be that this reasonable initial guess is often possible for the case of model parameter estimations since there often exists at least some experimental data in such cases. Considering all these conditions, as the first step, a non-derivative-type optimization algorithm, the so-called Simulated Annealing (hereinafter SA, e.g. Finsterle (1993) or Kobayashi (2004)) was selected. SA has some interesting characteristics as follows:

- (1) SA can escape from local extrema if it is well tuned;
- (2) SA does not require the calculation of the derivatives of the objective function, hence the coding is relatively easy;
- (3) As a result, SA is considered robust, irrespective of the shape of the objective function.

Other non-derivative-type methods were not selected since some of them are considered too simple and therefore they cannot escape from local extrema (e.g. trial and error, greedy search method); some are considered more complex in terms of coding (e.g. genetic algorithm, evolutionary algorithm); nevertheless, it is considered that the ultimate computational efficiency may not be so different. For these reasons, it is regarded that starting from the SA is logical enough.

Simulated annealing

The SA algorithm especially tailored for the following application is described as follows:

i: index for acceptance

j: index for rejection

k: index for the cooling schedule

$\vec{x}_c^{i,j,k}$: current decision vector

$\vec{x}_n^{i,j,k}$: new decision vector

$\vec{x}_{best}^{i,j,k}$: best decision vector

$obj(\vec{x}), obj_{best}^i$: Objective function and its best value

δ_j, \mathfrak{R}_j : random variables

$x_{max}, x_{min}, i_{max}, j_{max}$: boundary values for x, i, j

Choose $x_c^{0,0,0}$;

Compute $Obj(x_c^{0,0,0})$ by MUFTE–UG;

Set $i = 1, j = 0, k = 0$;

Repeat

{

Generate $f(\sigma^k, \mu)$, a random number

Compute $x_n^{i,j,k} = x_c^{i,j,k} + f(\sigma^k, \mu)\Delta x_c^{i,j,k}$

If $\{x_n^{i,j,k} > x_{max} \parallel < x_{min}\}$ go to generate $f(\sigma^k, \mu)$

Compute $Obj(x_n^{i,j,k})$ by MUFTE–UG

If $\{Obj(x_n^{i,j,k}) - Obj(x_c^{i,j,k}) = \Delta Obj > 0\}$

then $x_c^{i+1,j,k} = x_n^{i,j,k}$ and $Obj(x_c^{i+1,j,k}) = Obj(x_n^{i,j,k})$

Set $i = i + 1, j = j, k = k$;

else

Generate \mathfrak{R}_j , a random number $0 < \mathfrak{R}_j < 1$

If $\{\mathfrak{R}_j > P_{Bol}\}$

then $x_c^{i+1,j,k} = x_n^{i,j,k}$ and $Obj(x_c^{i+1,j,k}) = Obj(x_n^{i,j,k})$

Set $i = i + 1, j = j, k = k$;

else $x_c^{i,j+1,k} = x_c^{i,j,k}$ and $Obj(x_c^{i,j+1,k}) = Obj(x_c^{i,j,k})$;

Set $i = i, j = j + 1, k = k$;

If $\{i > i_{max} \parallel j > j_{max} = i_{max}/5\}$

then $i = 0, j = 0, k = k + 1$

}

until $\{k > k_{max}\}$

where $f(\sigma^k, \mu)$ stands for the normal distribution, σ^k the standard deviation in the k th iteration and μ the mean. As the cooling step proceeds, the standard deviation σ^k is reduced as (Finsterle 1993):

$$\sigma^k = \left(\frac{k_{max} + 10}{k_{max} + 11} \right)^k \sigma^0$$

where σ^0 is the standard deviation at the initial temperature, k_{max} the total number of cooling steps. Δx is calculated such that: $\Delta x = A(x_{bnd}^{up} - x_{bnd}^{low})$ where A is the coefficient determined by trial and error and x_{bnd} the boundary value of the decision vector. The superscripts *up* and *low* denote the upper (maximum) and lower (minimum) boundaries. The so-called Boltzmann probability in the chart as the criterion of the deteriorated solution acceptance is expressed by

$$P_{Bol} = e^{\left(\frac{-(Obj(x_{i+1}) - Obj(x_i))}{k_B T_k} \right)} = e^{\left(\frac{-\Delta Obj}{k_B T_k} \right)}$$

where $Obj(x)$ is the objective function, $\Delta Obj = Obj(x_{i+1}) - Obj(x_i)$ and T_k the temperature at the k th cooling stage. The cooling schedule is represented by $T_k = \alpha T_0$ where T_0 is the initial temperature and α the coefficient determined heuristically. There are several criteria considered to be reasonable in order to terminate the simulation. This time the optimization procedure is terminated after taking k_{max} number of cooling steps.

Objective function

In the following application, the objective function is defined as

$$Obj(x) = \max \sum_i^{num} Q_{m,i}(x_i)$$

where x_i is the coordinate of the well i constrained by the boundaries of the decomposed roadway, $Q_{m,i}$ the amount of the methane extracted from well i at the steady state located at the coordinate x_i and num the total number of wells. This objective function means that our optimal condition is the result of positioning extraction wells at the locations where the sum of the methane extractions is maximized. In other words, this objective function implies that we control the methane behavior focusing on its physics. The parameters of the simulation–optimization model tuned heuristically for the following application are summarized in Table 1.

Table 1 | The parameters for the optimization procedure

k_{max}	K_{Bol}	T_0	α	A	μ	σ^0
10	1	0.25	0.8	2/5	0	1/3

Simulation–optimization model coupling procedure

The coupling procedure of a mesh generator, MUFTE-UG and SA is outlined in Figure 2 (hereinafter referred to as MUFTE-SA). One feature here is that it includes the process of mesh generation by the mesh generator ART (Fuchs 1999). This was necessary because, in the subsequent application, the computational mesh is needed to be renewed in each simulation in order to install the extraction wells at different locations (see Figure 3). This means that the decision variables (i.e. the coordinates of the wells) are continuous under the limitation of the discrete (digital) nature of computers. The position of the installation is decided based on the response from the SA.

The overall procedure is described as follows. First, the initial input parameters necessary for MUFTE-SA are given. Then, the initial mesh is generated by ART based on the initial condition. Initial and boundary conditions are then assigned to the generated mesh according to the rules of the simulator MUFTE-UG, and the initial simulation starts. The objective function used in the optimization procedure is nothing less than the response of this simulation. Thus, the objective function calculated with the initial decision vector is obtained. Then, SA yields the next decision vector, ART generates the mesh based on SA results and MUFTE-UG computes the objective function for the next vector. After that, the current objective function is always compared with the previous objective function and the acceptance of the new solution is determined by the aforementioned Boltzmann probability. After repeating the same procedures, the optimization is terminated when it reaches a termination criterion. For further details, see Kobayashi (2004).

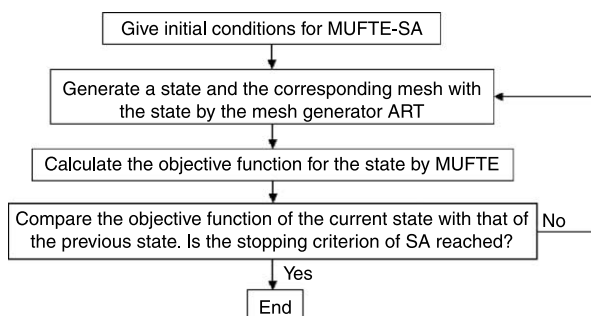


Figure 2 | Chart of the simulation–optimization procedure.

Parallelization scheme in optimization

The total CPU time often becomes huge when the simulation–optimization model is applied to real-world problems since the time is the sum of quite a few individual real-world simulations. Thus, in general parallel computing in terms of the simulation and/or the optimization is required (for the parallelization of MUFTE-UG, see, for example, Bastian & Helmig (1997)).

According to Sanchez & Frausto-Soils (2002), a parallel design of SA algorithms can be classified into the following two categories (for further details see, for example, Sanchez & Frausto-Soils 2000, Sanchez & Frausto-Soils 2002, Greening 1990 and Azencott 1992):

- Pseudo-parallel SA algorithms: sequential SA algorithms run on different processors at the same time or the data domain is assigned to different processors where a sequential SA is running.
- Parallel SA algorithms: the SA algorithm is divided into tasks which are distributed among several processors.

The parallelization scheme used in the subsequent application is from the first category, that is, a parallelization by means of domain decomposition. In this method, the simulation runs in the whole domain, while the optimization is carried out in the decomposed subdomains. Such a coarse-grain parallelization is comparatively easy to implement and leads to nearly ideal parallel speed-up, i.e. that the speed-up is nearly p for a parallel computation with p processors. An example of a parallelization design by such a domain decomposition tailored for the subsequent application is shown in Figure 4.

In the subsequent application, the total time was, even in the simplest case, expected to be around 7 h (each simulation CPU time) \times 1000 iterations/24 h = 292 d. Thus the use of a parallel computer was inevitable. This was realized by decomposing the roadway of the coal working into n segments (here $n = 23$; see Figure 4: the site details are described in the next section). After decomposing the roadway, k extraction wells are installed in k of the decomposed n segments with some reasonable assumptions from an engineering point of view. Afterwards, n simulation–optimization procedures are carried out on n CPUs of a parallel computer. Then, the (at least locally) optimal

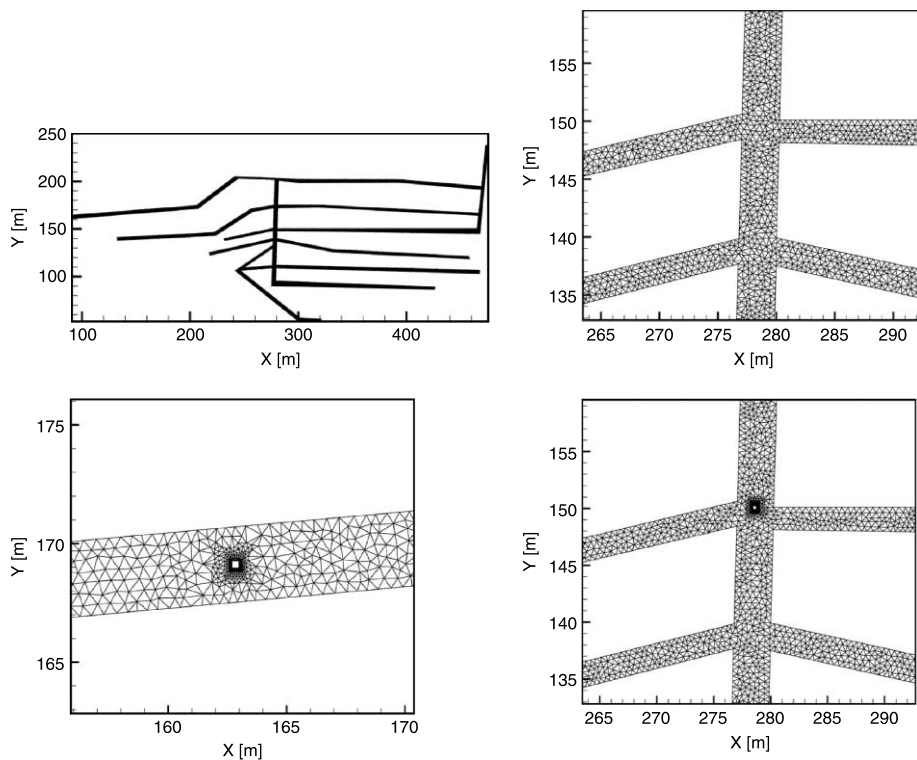


Figure 3 | Installation of extraction wells at different locations is realized by including the mesh generation process in the procedure (see Figure 2). Note that the rectangle indicates the extraction well. Top left: domain of mining site; top right: zoom into the mesh around crossings; bottom right: including a well into the mesh; bottom left: zoom into the mesh around the well.

solutions from n CPUs are collected in one processor to select one best solution among them. If the selected solution is considered to follow the stopping criterion, the entire procedure stops, otherwise it iterates with the same procedure. By doing this, the total time for the simplest case was expected to be reduced using 23 CPUs, by rough estimation, to $292 \text{ d}/23 = 12.7 \text{ d}$. This parallelization scheme is transferrable to many other applications such as finding the best locations of the observatory, etc., because the message passing procedures between CPUs of a parallel computer is limited, hence easy to be implemented.

MODEL APPLICATION TO A COAL MINING SITE

The aforementioned simulation–optimization model is then applied to a coal mining site in the Ruhr, Germany. Some related data set was provided by a German company in charge of the operation.

Description of the coal mining site

The coal mining site remains below ground and at present a furniture company is opening its store on the surface. Figure 5 shows a plan view of the coal mining site. In the figure, the roadways of the former coal working at a depth of 40 m are represented with the darker gray color, while the lighter gray color represents the coal working at a depth of 60 m. Figure 6 shows a schematic diagram of the transversal view of the site. This figure outlines the geological structure. As shown in the figure, the roadways at the two levels are surrounded by carbon layers. The six small dots in the plan view show the locations where so-called passive extraction wells are already installed. Passive means that no electric energy is supplied for use; instead the gas in the mine goes out to the surface via the well due to the pressure difference between the atmosphere (ca. 1 bar) and the underground pressure (ca. 1 bar + 10–100 mbar by observation). Figure 7 shows the appearance of one of the installed six passive extraction wells.

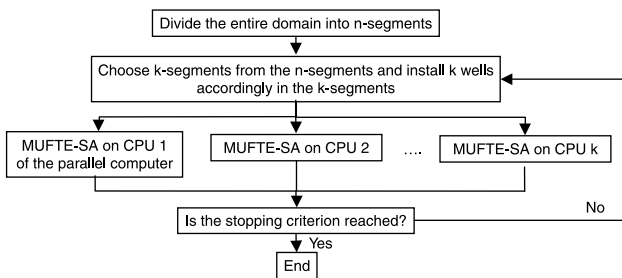
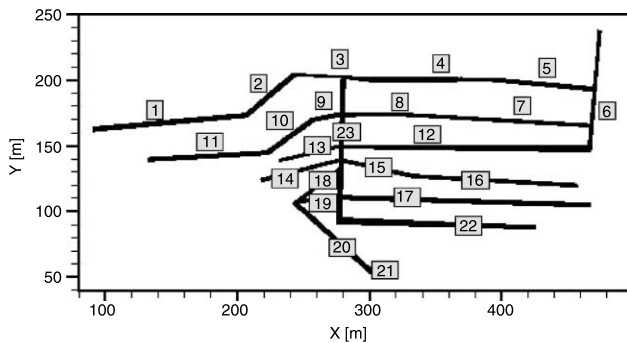


Figure 4 | 23 subdomains of the mining site (top); chart of the parallelization procedure by means of domain decomposition (bottom). Note that the simulation itself is carried out in the whole domain, while the optimization runs only in the subdomain.

At present, almost no information with regard to the real condition of the site is available except the measured permeability. A collapse of the surrounding strata in the roadways has most probably taken place, resulting in filling-in of the roadways; however, the exact state is not known. All that is known is that the methane adsorbed in the coal seams in the site is still continuously desorbed; thus it has to be extracted, in this case, by installing extraction wells. Therefore, the six passive extraction wells were installed

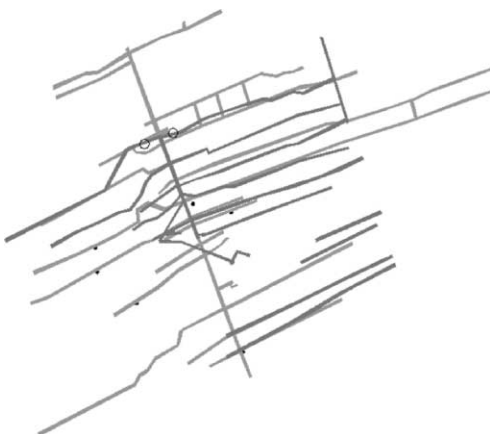


Figure 5 | Plan view of the coal mining site in the Ruhr, Germany. The black small dots indicate where the passive extraction wells are installed.

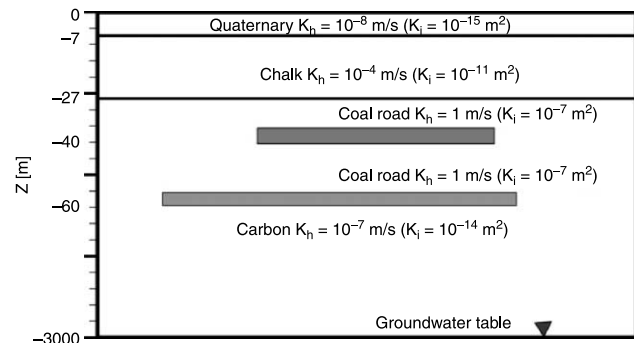


Figure 6 | Schematic diagram of the geological structure of the site.

mainly based on the intuition of experienced engineers. At this point, it was considered even better, in addition to their experience, if the manner of the installation could be reinforced by some assessments obtained from this simulation–optimization constrained by the quality of the available data. Along this line, the objective function was defined such as the one given in the section “Objective function”.

Simulation conditions

As the starting point of this application, it was decided to model only the upper level coal working at the level of $z = -40$ m in a horizontal 2D cut.



Figure 7 | A passive extraction well at the site.

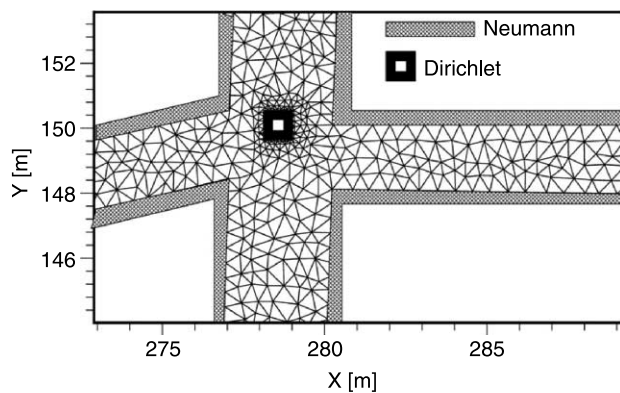


Figure 8 | The boundary condition for the simulation.

First, two assumptions are made; the methane is injected as a uniformly distributed source in the computational domain and the extraction well is represented as a rectangular hole 0.3 m on a side. Then, an attempt to model the entire working, not only the roadways but also the surrounding coal seams consistently, was made as shown in [Figure 9](#). However, other insights emerged at this point: the flow from the filled roadways to the surrounding coal seams does not always have to be taken into account because the differences of the permeabilities between these two media are large enough (from observation, the absolute permeability of the filled roadway is 10^{-7} m^2 , compared to that of the matrix of 10^{-14} m^2). Thus, the inclusion of the surrounding coal seams is temporally suspended.

One point coming from this assumption would be that this may change the time until the system reaches steady state. However, it was considered that it would not influence the suboptimal locations of the wells. Moreover, the discrepancy of the time span in this case is considered as of minor importance since the well maintenance cost is not

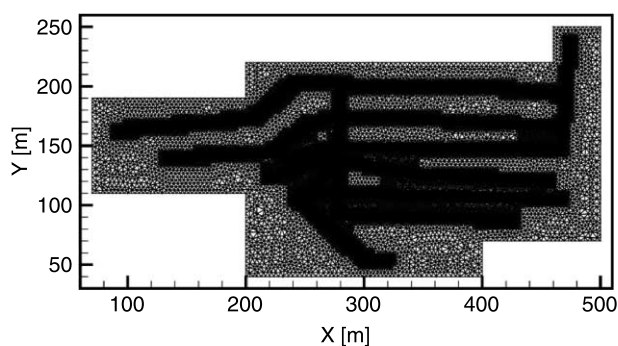


Figure 9 | Generated mesh including the surrounding coal seams.

that high, and additionally the real distribution of the unexploited coal seam is not known due to lack of information.

The computational mesh and the boundary conditions for such a case are shown in [Figure 8](#). The methane release from the surrounding coal seams is expressed by the influx as a Neumann boundary condition at the roadway boundary. The amount of the influx per unit length from the boundary is $q_{node}^{tot} = 6.59 \times 10^{-4} \text{ mol/ms}$, totally equivalent to the $q_{node}^{tot} \times L = q^{tot} = 2.506 \text{ mol/s}$ where L is the total length of the roadway boundary. This amount equals $q^{tot} = 225 \text{ m}^3/\text{s}$ under atmospheric pressure condition, almost corresponding to the observational data provided by the German company. It is assumed that the influx contains 80% methane, 19% air and 1% water. This assumption comes from the fact that the methane composition of the extracted gas from already installed wells never attains a value more than 80%. The passive extraction is expressed by setting the gas phase pressure to 1 bar, i.e. atmospheric pressure.

Simulation–optimization results

This section describes the results of the simulation–optimization application for one, two and three well installations. For the reduction of the CPU time, it is decided to carry out each simulation for only around 7 h of the complete around 14 h simulation in the application since some preliminary tests showed that the optimal locations basically do not differ by this arrangement (see [Kobayashi \(2004\)](#) for further details).

One-well installation

For this one-well installation, 23 independent simulation–optimizations are carried out in the 23 decomposed subdomains and those 23 locally optimal results are eventually sent to one processor to evaluate the overall optimal result. As a result, two almost-equally optimal locations, one in segment 23 and the other in segment 14, are found. The gas pressure field when the well is located at the suboptimal place in segment 23 is shown in [Figure 10](#) (left). [Figure 10](#) (right) shows the percentages of the gas extraction amounts relative to the total gas influx at the

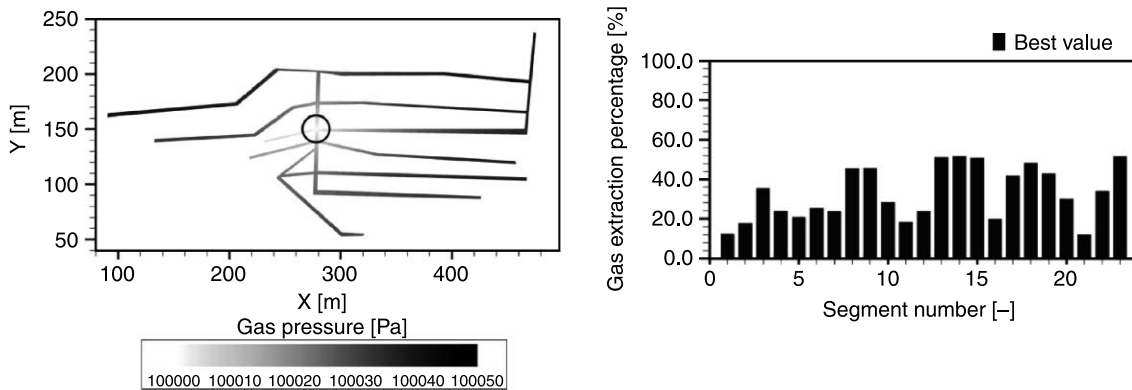


Figure 10 | Gas pressure field when the well is installed at the suboptimal position in segment 23 (left) after 40 s. Percentages of the gas extraction amounts to the total gas influx in the suboptimal location of each segment (right).

suboptimal locations in one of the 23 segments. Note that the percentage attains at most around 50% since the simulations were terminated around that time.

First, it is recognized that the suboptimal location in each segment is generally found at the crossing of several roadways. From the shape of the coal working, in many cases those points exist in central segment 23. As shown in Figure 10 (right), the well at the suboptimal location either in segment 14 and 23 extracts already around 50% equivalent of the gas influx at this stage, while the worst among the suboptimals only do around 12.5% (e.g. segments 1 and 21). Note that the difference between the best and worst values in this application becomes greater if the worst value from segment 1 and the best value from segment 23 are considered.

Second, as a general tendency, the segments connected to the central segment 23, such as segments 3, 8, 9, 13, 14, 15, 17, 18, 19 and 22, always realize better extractions. Thus, it is considered natural, based on these consequences, that the well at the crossing can extract gas from the surroundings much easier than the well at a place where the surroundings are bounded by the walls of the roadway can.

Two-well installation

The difficulty when installing more than one well is that, for instance in the two-well case, all possible combinations of the two-well installation by selecting 2 out of the 23 segments mean that $22 \times 23/2 = 253$ combinations exist;

hence it is expected that the total computational time, even using all 56 CPUs of the parallel computer, would be $253 \times 292 \text{ d}/56 \text{ nodes} = 1319 \text{ d}$. In other words, it is not practical and reasonable. Therefore, it is decided to use the constraint that one well only is installed in the central segment 23. This constraint is determined mainly based on the insights from the previous one-well case such that it has been clearly shown that the gas extraction is always better realized when the well is installed in or near the vicinity, especially at the crossings of the central segment 23. By introducing this constraint, the total time is expected to be almost the same as the one-well installation.

Henceforth the two wells are called well 1 and well 2. Well 1 is installed in one of the 23 segments, while well 2 is always in segment 23. As a result, two suboptimal situations, as in the previous one-well case, are found as shown in Figure 11. The left figure shows the case when well 1 is installed in segment 23, while the right figure shows when well 1 is installed in segment 6. Then, the bottom figure attempts to clarify the differences between these two suboptimal situations by showing the total amounts of gas extraction in these two cases and the extractions from well 1 in segment 23 and well 2 in segment 23, on the one hand, and well 1 in segment 23 and well 2 in segment 6, on the other hand. Apparently, the gas extraction either from well 1 or well 2 for the segments 23 and 23 combination is, on average, lower than that from well 2 for the segments 6 and 23 combination. This fact indicates that the considerable higher interaction between those two wells both in segment 23 for the segments 23 and 23 combination prevents the

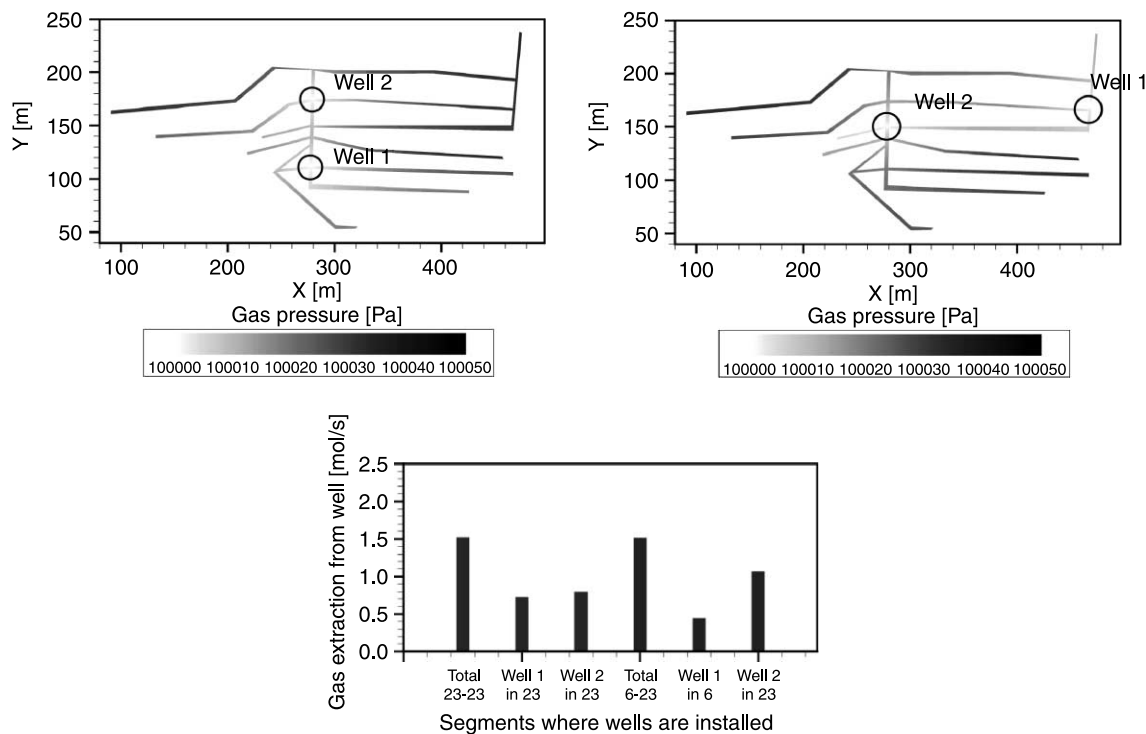


Figure 11 | Gas pressure field when the well is installed at the suboptimal location either in segments 23 and 23 (above left) or in segments 6 and 23 (above right) after 33 s. Bottom figure shows the total gas extraction from those two wells and the gas extractions from well 1 or well 2 when well 1 is installed in segment 23 or in segment 6.

extraction from each well, while the interaction for the segments 6 and 23 combination is lower because the distance between the wells is much larger, actually one of the largest among all the segments i -23 combinations ($i = 1, \dots, 23$).

Three-well installation

For the case of a three-well installation, two out of the three wells are installed in the central segment 23. This is based on the fact that for the two-well case the two wells both installed in segment 23 have realized one of the suboptimal extractions. This implied that this pattern plus the third well somewhere in the segment i ($i = 0, \dots, 23$) would produce one of the suboptimal values even if it would not be the very best among all combinations. Henceforth, the well in segment i is called well 1 and the other two wells in segment 23 are well 2 and well 3.

Figure 12 shows the gas pressure fields in the two suboptimal cases. The first one is realized by installing those three wells in segments 6, 23 and 23 (above left), while

the pattern of installing those three wells in segment 23 (above right) shows a slightly worse result than the segments 6–23–23 combination. The bottom figure shows the total gas extractions for both cases, and the extraction from one of the three wells installed either in segments 6, 23, 23 or 23, 23, 23, respectively. As can be seen, wells 2 and 3 for the segments 6, 23 and 23 combination realize better extraction than those for the segments 23, 23 and 23 combination, although well 1 shows the opposite result. As the sum, two relatively higher extractions from wells 2 and 3 plus a lower extraction from well 1 for the segments 6, 23 and 23 combination realize in total a better extraction than three well installation all in segment 23 when the extraction from each well is restrained due to the strong interactions.

Summary

Some general suggestions for solving this kind of extraction well installation problem are as follows:

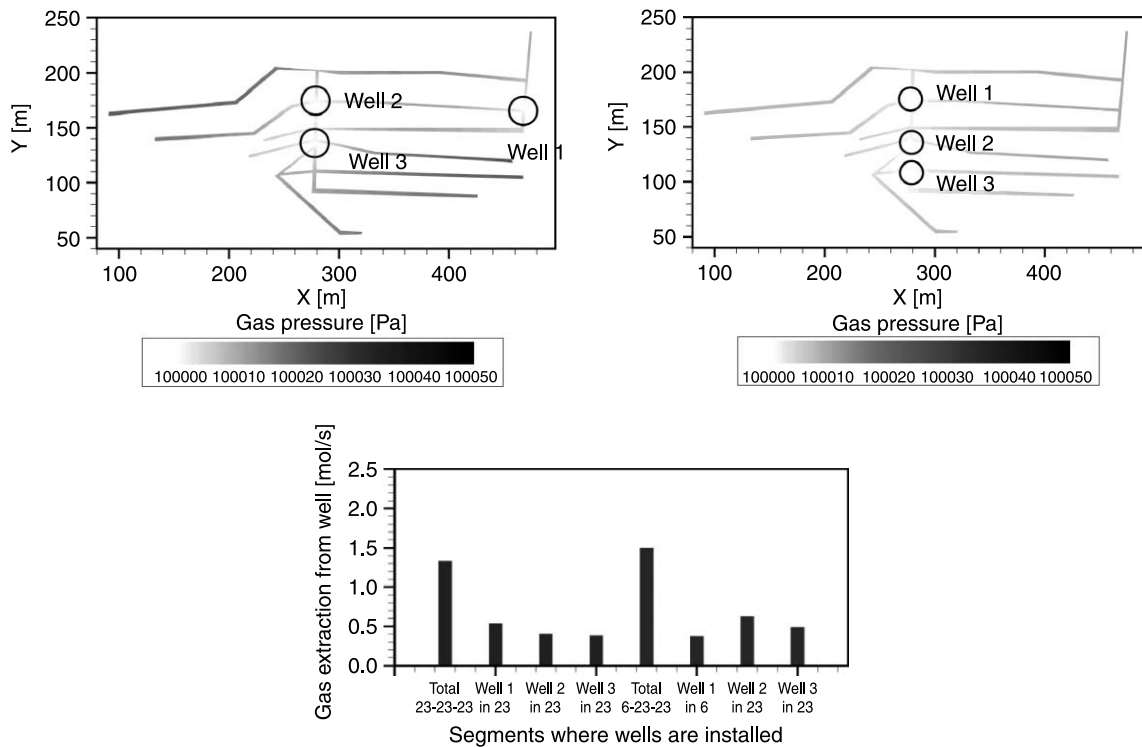


Figure 12 | Pressure field when those three wells are installed in segments 6, 23 and 23 (above left) and in segment 23 (above right) after 20.5 s. Bottom figure shows the total gas extraction and the gas extraction from one of the three wells when the three wells are installed in segment 23, and in segments 6 and 23.

- Generally, the total gas extraction becomes large when the wells are installed at places where several roads meet (i.e. at crossings), although the gas extraction from a well is restrained by other wells if the distances between these wells are too short. Thus, in the case when the site information is not available enough, it is recommended to install the wells firstly at the crossings, keeping in mind that the distances between the wells at those crossings should be taken as large as possible.

Secondly, the suggestion considered specific to this site are summarized as follows:

- From the configuration of the site, the gas extraction is generally large when the well is installed at the crossings of the central segment 23 since the surrounding gas is accumulated most easily and quickly. This is important in that, even though the assumptions made for the simulation herein do not hold in reality (e.g. the source is not uniformly distributed), there is still a greater possibility of better extraction by installing the wells in the central segment. This is considered much more reasonable than installing

the wells by engineers' intuition in case the site information is not available and further investment is not anticipated.

- The best gas extractions in one- and two-well cases are realized by installing the wells at the crossings in the central segment, albeit this does not hold for the three-well case. For the three-well installation, two wells in the central segment and the other one in the segment farthest from the central segment achieved the best extraction.

CONCLUSIONS AND FUTURE ASPECTS

This paper has shown the applicability of a new simulation–optimization model especially tailored to study the optimal management strategy of a closed coal mine in the Ruhr, Germany. The simulation–optimization model automatically controls the multiphase/multicomponent flow simulation; the optimization model (Simulated Annealing); the mesh generation function; the coupling of them; and the use of a parallel computer to handle the considerable CPU time. As an instance of real-world applications, the optimal

management strategy of a closed coal mine in the Ruhr, Germany was dealt with.

One distinct feature in this research was this aspect that the newly developed model has shown that it can compulsorily yield a solution of a kind even if the Simulated Annealing used herein would not be the very best. This is considered reasonable in one sense since it is often the case that the best approach is not known in advance, especially at the initial stage of less experienced fields. As a result of this application, especially of having carried out the enormous number of simulations for possible system combinations, it is considered that some gradient type methods are also applicable.

However, it is still important to remember that these gradient type methods do not always guarantee to yield a better solution than SA does, especially if the number of wells increases or the site configuration becomes more complex. Therefore, this kind of approach, i.e. the simulation of all (most) the considerable assortment is probably inevitable in some cases. Whether or not accepting these burden depends mainly on the importance of the problem.

Thus, it should be noted that there is always a trade-off between the accuracy and the total CPU time. As the methods used here are pretty general, this model is considered easily transferrable to many applications such as finding the best locations for the observatory.

The suggestions made here are rather simple and therefore they are applicable in other locations to improve operations. Moreover, the rules are, nevertheless, much more logical than human intuitions when the site information is not enough and further investment is not expected due to its termination.

ACKNOWLEDGEMENTS

This work was carried out during the first author's stay at the University of Stuttgart, Germany. During that time, this work was supported by the European Coal and Steel Community Research and Technology Development Program and the Deutsche Montane Technology GmbH. The authors had fruitful discussions with C. Shoemaker from Cornell University and S. Finsterle from the Lawrence

Berkeley National Laboratory, University of California. The authors would like to thank all of them.

REFERENCES

- Aly, A. H. & Peralta, R. C. 1999 Optimal design of aquifer cleanup systems under uncertainty using a neural network and a genetic algorithm. *Wat. Res. Res.* **35** (8), 2523–2532.
- Azencott, R. 1992 *Simulated Annealing; Parallelization Techniques*. John Wiley and Sons, New York.
- Bastian, P. & Helmig, R. 1997 Efficient fully-coupled solution techniques for two-phase flow in porous media, 2. Parallel multigrid solution and large scale computations. *Adv. Wat. Res.* **23**, 199–216.
- Doherty, J. 2002 Groundwater model calibration using pilot points and regularization. *Ground Water* **41** (2), 170–177.
- Finsterle, S. 1993 *Itouch2 User's Guide*. Lawrence Berkeley National Laboratory, University of California, Berkeley, CA.
- Finsterle, S. 2000 *Demonstration of Optimization Techniques for Groundwater Plume Remediation*. Project report 46746, Lawrence Berkeley National Laboratory, University of California, Berkeley.
- Finsterle, S. & Pruess, K. 1995 Solving the estimation-identification problem in two-phase flow modeling. *Wat. Res. Res.* **31**, 913–924.
- Fuchs, A. 1999 *Optimierte Delaunay-Triangulierungen zur Vernetzung getrimmter NURBCs-Koerper*. PhD dissertation, ShakerVerlag, Aachen.
- Greening, D. 1990 Parallel simulated annealing techniques. *Physica D* **2**, 293–306.
- Helmig, R. 1997 *Multiphase Flow and Transport Processes in the Subsurface*. Springer, Berlin.
- Helmig, R., Jakobs, H., Bastian, P. & Reichenberger, V. 2000 *Multiphase Multicomponent Processes in Fractured Porous Media*. Project report 6, Technische Universität Carlo Wilhelma zu Braunschweig, Institut für ComputerAnwendungen im Bauingenieurwesen.
- Hinkelmann, R. 2005 *Efficient Numerical Methods and Information-processing Techniques for Modeling Hydro- and Environmental Systems*. Springer, Berlin.
- Hinkelmann, R., Breiting, T., Kobayashi, K., Helmig, R. & Sheta, H. 2004 Application of hydroinformatic methods and techniques for complex systems. In *Quantification of Methane Migration Processes from Abandoned Coal Mines*, (ed. S. Y. Liang, K. K. Phoon & V. Babovic), World Scientific, Singapore, vol. 1, pp. 222–229.
- Kobayashi, K. 2004 *Optimization Methods for Multiphase Systems in the Subsurface –Application to Methane Migration in Coal Mining Areas*. Institut für Wasserbau, Universität Stuttgart, Germany, Mitteilungsheft 139.
- Kobayashi, K., Hinkelmann, R. & Helmig, R. 2003 Comparison of different model concepts for gas-water processes in the subsurface. In *Proc. XXX IAHR Congress, Thessaloniki, Greece, 24–29 August 2003* (ed. J. Ganoulis, P. Prinos, C. Maksimovic & V. Kaleris), CD-ROM.

- McDonald, M. & Harbaugh, A. 1988 *A Modular Three-dimensional Finite Difference Groundwater Flow Model*. US Geological Survey, Virginia, US Geological Survey Water Resources Investigations, Book 6, chap. A1.
- McPhee, J. & Yeh, W. W. -G. 2004 **Multiobjective optimization for sustainable groundwater management in semiarid regions**. *J. Wat. Res. Plann. Mngmnt.* **130**, 490–499.
- Maskey, S., Jonoski, A. & Solomatine, D. P. 2002 **Groundwater remediation strategy using global optimization algorithms**. *J. Wat. Res. Plann. Mngmnt.* **128**, 431–440.
- Nunes, L. M., Cunha, M. C. & Ribeiro, L. 2004 **Groundwater monitoring network optimization with redundancy reduction**. *J. Wat. Res. Plann. Mngmnt.* **130**, 33–43.
- Poeter, E. & Hill, M. 1998 *Documentation of UCODE, A Computer Code for Universal Inverse Modeling*. US Geological Survey, Virginia, Project report, US Geological Survey Water Resources Investigation Report 98-4080.
- Sanchez, S. H. & Frausto-Soils, J. 2000 A methodology to parallel the temperature cycle in simulated annealing. In *MICAI 2000. LNAI 1973* (ed. O. Cairo, L. E. Sucar & F. J. Cantu), Springer-Verlag, Berlin, pp. 63–74.
- Sanchez, S. H. & Frausto-Soils, J. 2002 MPSA - A Methodology to Parallelize Simulated Annealing and Its Application to Traveling Salesman Problem. *Lectures Notes on Computer Science* **2313**, 89–97.
- Zheng, C. 1990 *MT3D, A Modular Three-dimensional Transport Model for Simulation of Advection, Dispersion and Chemical Reactions of Contaminants in Groundwater System*. Available at: http://hydro.geo.ua.edu/mt3d/mt3d_1990.pdf USEPA, Oklahoma, USA.

First received 21 December 2006; accepted in revised form 24 August 2007